Published in final edited form as:
Biochem J. 2008 December 15; 416(3): 347–355. doi:10.1042/BJ20080165.

Mfsd2a encodes a novel major facilitator superfamily domain-containing protein highly induced in brown adipose tissue during fasting and adaptive thermogenesis

Martin Angers[1], **Marc Uldry**[2], **Dong Kong**[3], **Jeffrey M. Gimble**[4], and **Anton M. Jetten**[1,*]

1*Cell Biology Section, LRB Division of Intramural Research National Institute of Environmental Health Sciences National Institutes of Health 111 T.W. Alexander Drive Research Triangle Park, NC 27709*

2*Dana-Farber Cancer Institute Harvard Medical School 1 Jimmy Fund Way Boston, MA 02115*

3*Division of Endocrinology, Department of Medicine Beth Israel Deaconess Medical Center and Harvard Medical School 99 Brookline Ave Boston, MA 02215*

4*Stem Cell Laboratory Pennington Biomedical Research Center Louisiana State University System 6400 Perkins Rd, Baton Rouge, LA 70808*

Abstract

This study describes the identification of a novel mammalian major facilitator superfamily domain-containing protein, referred to as Mfsd2a, and an additional closely related protein, designated Mfsd2b. Most intron/exon junctions are conserved between the two genes suggesting that they are derived from a common ancestor. Mfsd2a/b share a 12 transmembrane α-helical domain structure that shows greatest similarity to that of the bacterial Na^+/melibiose symporters. Confocal microscopy demonstrated that Mfsd2a localizes to the endoplasmic reticulum. *Mfsd2a* is expressed in many tissues and is highly induced in liver and brown adipose tissue (BAT) during fasting. *Mfsd2a* displays an oscillatory expression profile in BAT and liver consistent with a circadian rhythm. While the basal level of *Mfsd2a* expression is relatively low in BAT in mice, it is greatly induced during cold-induced thermogenesis and after treatment with β-adrenergic receptor (βAR) agonists. This induction is totally abolished in βAR-deficient (β-less) mice. These findings indicate that *Mfsd2a* is greatly up-regulated in BAT during thermogenesis and that its induction is controlled by the βAR signaling pathway. The observed induction of *Mfsd2a* expression in cultured BAT cells by dibutyryl-cAMP is in agreement with this conclusion. Our study suggests that *Mfsd2a* has a role in adaptive thermogenesis.

Keywords

Symporter; permease; thermogenesis; brown adipose tissue

INTRODUCTION

Energy homeostasis can be defined as the maintenance of the delicate balance between energy intake and energy expenditure. Brown and white adipose tissues (BAT and WAT) play important but opposite roles in energy homeostasis [1,2]. The major and most efficient way to store excess energy is in the form of triglycerides (TG), which are primarily stored in WAT [3]. This energy can be released during times of energy deprivation. TG are then hydrolyzed

*To whom correspondence should be addressed Tel: 919-541-2768; Fax: 919-541-4133 E-mail: jetten@niehs.nih.gov

into free fatty acids which are then mobilized to peripheral tissues where they can be directly oxidized to generate energy for cellular and organ functions, physical activity, and adaptive thermogenesis. Cold-induced thermogenesis involves increased thermal energy output in skeletal muscle and BAT [4-7]. BAT converts the energy stored in TG into heat by uncoupling the ATP production from respiration a process known as non-shivering thermogenesis.

The β^3-adrenergic signaling pathway has been demonstrated to play a key role in the control of adaptive thermogenesis in rodents; however, this process appears to be less important in humans [4,5,8]. In response to cold exposure, the sympathetic nervous system releases norepinephrine (NE) to interact with β-adrenergic receptors (βAR) expressed on the surface of brown adipocytes. This activation elevates intracellular cAMP levels, increases the rate of lipolysis, and induces the expression of multiple genes, including uncoupling protein 1 (*UCP1*) and deiodinase 2 (*DIO2*) [6,7,9]. Oxidation of free fatty acids ultimately leads to the creation of a proton electrochemical gradient [4,5,8]. Under β-adrenergic stimulation, UCP1 uncouples this energy from the synthesis of ATP and instead promotes its conversion into heat.

In addition to βAR, a number of different transcription factors and co-factors, including cAMP-responsive element binding protein (CREB), the nuclear respiratory factors (NRFs) 1 and 2, and several nuclear receptors, have been implicated in the regulation of genes expression during adaptive thermogenesis [4,10-13]. Recent studies have shown that PPARγ-coactivator 1α (PGC-1α) plays a critical role in the regulation of gene expression during thermogenesis [13, 14].

In the present study, we describe the identification of a novel member of the major facilitator domain-containing family, referred to as Mfsd2a. Sequence comparison identified an additional related protein, not previously reported and designated Mfsd2b. Both Mfsd2 proteins exhibit sequence and structural similarities with bacterial permeases and symporter proteins suggesting that they are members of the major facilitator superfamily. We examined the regulation of *Mfsd2a* during brown fat differentiation, adaptive thermogenesis, and fasting. Our results indicate that *Mfsd2a* is greatly up-regulated in BAT during thermogenesis and that its induction is controlled by the βAR signaling pathway. This is supported by the induction of *Mfsd2a* expression in cultured BAT cells by dibutyryl-cAMP (dibut-cAMP). These data are consistent with the conclusion that activation of the βAR signaling pathway plays a major role in the induction of *Mfsd2a* expression during adaptive thermogenesis.

MATERIAL AND METHODS

Experimental animals

C57BL/6 RORα$^{sg/sg}$RORγ$^{-/-}$ double knockout (DKO) mice, deficient in the expression of the retinoid-related orphan receptors RORα and RORγ, and mice deficient in the expression of all three β-adrenergic receptors (β-less AKR/J mice) were described previously [15,16]. Mice were individually housed at 22°C and maintained on a constant 12 h light: 12 h dark cycle with the light cycle beginning at 6 AM. In some experiments mice were exposed to cold (4°C) for up to 8 h or fasted for 16 h starting at the onset of the dark cycle. Mice were fed NIH-A31 chow and water *ad libitum*. In experiments with β-agonist treatment, mice were injected intraperitoneally with 100 mg/kg isoproterenol (I5627; Sigma, St-Louis, MO), 1 mg/kg CL316243 (C5976; Sigma) or saline (control). During fasting mice had unlimited access to water. All animal protocols followed the guidelines outlined by the NIH Guide for the Care and Use of Laboratory Animals and were approved by the Institutional Animal Care and Use Committee at the NIEHS and Harvard Medical School.

Plasmids

The mouse *Mfsd2a* sequence was submitted to Genbank under accession # AY880264. The genomic structure was deduced from the alignment of sequences # AY880264 and AK028886 with the mouse genomic DNA sequence (Genbank accession # AC125518.3) containing the entire *Mfsd2a* gene. *Mfsd2a* was amplified by PCR from a cDNA clone (Image clone ID # 5707105; Open Biosystems, Huntsville, AL) with a forward primer (5′-TTgAATTccccgcgggTcATggccAAAg-3′) and a reverse primer (5′-TTggATccgAgAATAcTggccAgcTcTg-3′) containing an *Eco*RI and a *Bam*HI restriction sites, respectively. The PCR product was cloned between the *Eco*RI and *Bam*HI restriction sites of the expression vector pCMV-3xFLAG-14 (Sigma), placing FLAG in frame at the C-terminus of Mfsd2a. The sequence was verified by restriction enzyme analysis and DNA sequencing.

BAT cell culture

Immortalized WT and PGC-1α KO brown fat adipocytes were described previously [14] and grown in pre-adipocyte medium (DMEM, 20% FBS, and penicillin/streptomycin). When cells reached confluence, medium was replaced with adipocyte medium (DMEM, 10% FBS, 20 mM HEPES, pH 7.4, 20 nM insulin, and 1 nM T_3) containing 0.5 mM isobutylmethylxanthine, 1 μM dexamethasone, and 0.125 mM indomethacin to promote differentiation. After 2 days of incubation, the medium was switched to adipocyte medium only for an additional 5 days. The medium was renewed every other day. Fully differentiated BAT cells (7 days after induction) were treated with 0.5 mM dibut-cAMP or 5 μM NE.

RNA isolation

Tissues, including abdominal WAT and interscapular BAT, were promptly isolated and kept overnight at 4°C in RNA*later*® solution (Ambion, Austin, TX). The following day, the tissues were removed from the RNA*later*® solution and stored at −80°C until used. Tissues were homogenized with a polytron PT 3000 (Brinkmann Instruments, Westbury, NY) in 2 ml of RLT solution (Qiagen, Valencia, CA) containing β-mercaptoethanol. The homogenate was then loaded into a QIAschredder™ column (Qiagen) and centrifuged at 17,000 × *g* for 3 min. The supernatant was mixed with one volume of ethanol 70% (50% for liver) and RNA isolated with the RNeasy® mini or midi kits (Qiagen) following the manufacturer's instructions. Total RNA from cells was isolated with TRI Reagent® (Molecular Research Center, Inc., Cincinnati, OH) according to the manufacturer's instructions.

Northern blot analysis

Total RNA (15 μg) was separated on a 1.2% agarose/5% formaldehyde gel in 1X MOPS buffer, transferred to a nylon membrane (Sigma), and subsequently UV cross-linked. The membranes were hybridized to ^{32}P-labeled cDNA probes specific for *Mfsd2a*. Hybridizations were performed at 68°C for at least 3 h. The membranes were then washed twice with 2X SSC and 0.1% SDS for 20 min at 22°C, and subsequently with 0.1X SSC and 0.1% SDS for 15 min at 50°C. Autoradiography was carried out at −70°C using Hyperfilm (Amersham Biosciences, Piscataway, NJ).

Microarray analysis

Total RNA isolated from BAT of WT and DKO mice was amplified using Agilent Low RNA Input Fluorescent Linear Amplification Kit following the manufacturer's protocol. Gene expression analyses were conducted by the NIEHS Microarray Group (NMG) on Agilent mouse 20,000-oligo chips as described previously [16]. The data discussed in this publication have been deposited in NCBIs Gene Expression Omnibus at http://www.ncbi.nlm.nih.gov/geo/query/acc.cgi?token=bfohfqeyyqikipy accession # GSE9969 .

Quantitative Real-time PCR (qRT-PCR)

Total RNA was first reverse-transcribed into cDNA with a High Capacity cDNA Archive Kit (Applied Biosystems, Foster City, CA) according to the manufacturer's instructions. QRT-PCR reactions were then carried out in triplicate with a 7300 Real Time PCR system (Applied Biosystems) using either the TaqMan® Universal PCR Master Mix (Applied Biosystems) or the RT^2 Real-Time™ SYBR Green/ROX PCR Master Mix (Superarray, Frederick, MD). Fifty ng of cDNA were used in each reaction to quantify the various gene expression levels, while 25 pg/reaction were used to measure 18S levels. Briefly, cDNA was denatured for 10 min at 95°followed by 40 cycles consisting of 15 s at 95°C and 60 s at 60°C. The average threshold cycle (Ct) values from triplicate PCR reactions for every genes were normalized against the Ct values obtained from the 18S transcript or cyclophilin B, which served as internal controls. The r^2values of each appropriate standard curves scored above 0.99. Pre-designed Assays-on-Demand™ primers/probe sets were purchased from Applied Biosystems while all other primers and probes were designed in-house using the Primer Express 2.0 software and synthesized by Sigma/Genosys. The sequence of the primers and probes are shown in Supplementary Table S1.

Confocal microscopy

Brown fat adipocytes or COS-1 cells (1,000 cells/cm^2) were plated in glass-bottom culture dishes (MatTek Corp., Ashland, MA) and transfected 24 h later with pCMV-Mfsd2a-3xFLAG-14 (0.2 μg) using FuGENE 6 (Roche Applied Science, Indianapolis, IN) according to the manufacturer's instructions or calcium phosphate precipitation. Cells were co-transfected with pDsRed2-ER (Clontech, Mountain View, CA) or stained with either MitoTracker Red CMX-Ros or LysoTracker Red, (Molecular Probes) to identify the endoplasmic reticulum (ER), mitochondria, and lysosomes, respectively. After 48 h, cells were fixed in 4% paraformaldehyde for 20 min and then permeabilized with 0.3% Triton X-100. After a 15-min incubation in SuperBlock® Blocking Buffer (Pierce, Rockford, IL), cells were incubated for 3 h with mouse anti-FLAG M2 antibody (Sigma) and 30 min with goat anti-mouse Alexa 488 (Molecular Probes, Eugene, OR). Nuclei were stained with 4′-6-diamidino-2-phenylindole (DAPI, Sigma). Fluorescence was observed in a Zeiss LSM 510 NLO confocal microscope (Zeiss, Thornwood, NY).

Statistical analysis

The qRT-PCR data were analyzed by Student's *t*-test. QRT-PCR expression levels are presented as mean ± S.E.

RESULTS

Identification of Mfsd2a

The nuclear receptors RORα and RORγ are both expressed in BAT [17]. To obtain insights into the function of these receptors in this tissue, we compared the gene expression profiles between WT and RORα/γ DKO mice by microarray analysis. This comparison identified a novel gene that was expressed at significantly higher levels in BAT from ROR-DKO mice. The gene encoded a 59 kDa protein not reported previously. The nucleotide and amino acid sequences are shown in Supplementary Figure S1A. The analysis of both sequence and the domain structure indicated that this protein is related to the Na^+/melibiose symporter and other related bacterial carbohydrate transporters/permeases (Figure 1), suggesting that it is a member of the major facilitator/sugar transporter family [18-21]. We refer to this protein as major facilitator superfamily domain-containing protein 2a (Mfsd2a).

Comparison of the mouse Mfsd2a protein sequence with sequences in Genbank (Blastn) identified the human homolog (Genbank accession # BAD38634). The sequence of Mfsd2a is highly conserved among species; mouse and human Mfsd2a proteins are ~85% identical (Figure 1). In addition, Mfsd2a showed high sequence homology with a sequence of another previously unreported protein closely related to Mfsd2a (Genbank accession # AK172423 and NP_001073942 for the mouse and human homolog, respectively). This protein, referred to as Mfsd2b, consists of 494 amino acids and exhibits a 59% similarity and a 42% identity with Mfsd2a (Figure 1). Additional sequence analysis showed that Mfsd2a exhibited a 68% identity and 80% similarity with the sequence of an unpublished *Xenopus laevis* protein (Genbank accession # AAI23089) and a 61% and 64% identity with two previously unpublished zebrafish (*Danio rerio)* proteins (Genbank accession # NP_001007452 and CAK04287) suggesting that they represent the *Xenopus* and zebrafish homologs of Mfsd2a (Figure 1). Sequence comparison revealed that both Mfsd2a and Mfsd2b are only distantly related to other mammalian transporters. The highest sequence similarity was found between Mfsd2a/b and the Na^+/melibiose symporter MelB [18-20] from several different bacteria, including those of the cyanobacterium *Nostoc punctiforme* (Genbank accession # ZP_00109128; 47% similarity) and the proteobacterium *Escherichia coli* (Genbank accession # ZP_00721556; 43% similarity), and several related carbohydrate transporters (Figure 1). The phylogenetic relationship between these proteins is shown in Supplementary Figure S1B. Based on their sequence similarities, it was concluded that the *Xenopus* and zebrafish proteins are more closely related to Mfsd2a than Mfsd2b.

Alignment of mRNA and genomic sequences revealed the genomic structure of the mouse *Mfsd2a* gene (Supplementary Figure S1C). The *Mfsd2a* gene spans about 14.3 kb and consists of 14 exons and 13 introns, while the *Mfsd2b* gene consists of 13 exons and 12 introns. All intronexon junctions are conserved between the *Mfsd2a* and *Mfsd2b* genes, except those associated with intron 6. In addition, *Mfsd2a* contains one extra intron (intron 9). This similarity in genomic structure suggests that *Mfsd2a* and *Mfsd2b* are derived from a common ancestral gene. The mouse and human *Mfsd2a* genes map to chromosome 4D2.2 and 1p33, respectively, while the mouse and human *Mfsd2b*genes map to 12A1.1 and 2p23, respectively.

Putative transmembrane domain structure

Although Mfsd2a exhibits only 43-47% sequence similarity with the Na^+/melibiose symporter MelB and related bacterial carbohydrate transporters, prediction analysis of the transmembrane helix domain structure of Mfsd2 proteins by http://www.cbs.dtu.dk/services/TMHMM-2.0/, http://www.predictprotein.org/, and http://bioweb.pasteur.fr/seqanal/interfaces/toppred.html indicated that their domain structures are strongly conserved. Previously reported topological studies of MelB have demonstrated that it contains 12 α-helical transmembrane domains (TMDs) [18-20,22,23]. Based on our topological analysis and comparison with MelB, it was predicted that Mfsd2a contains 12 putative α-helices (Figure 1), each α-helix containing at least 17 amino acids in agreement with the concept that they function as TMDs. The putative secondary structure of Mfsd2a and MelB proteins are compared in Figure 1. The similarities between the secondary structures of Mfsd2a and MelB support the conclusion that Mfsd2a also contains 12 TMDs.

As predicted by the similarities in their genome structure and sequence, the α-helices of Mfsd2a align with those of Mfsd2b (Figure 1). This analysis supports the assumption that both Mfsd2a and Mfsd2b function as membrane proteins and are members of the major facilitator superfamily. Several regions within Mfsd2a and Mfsd2b are highly conserved between each other and between various species suggesting they might have a functional role. These residues include: GRLMPW overlapping TMD 3, VPYSALTMF in TMD 4, ERDSATAYRMT in the loop between TMDs 4 and 5, GFLFTSLA in TMD 7, LTRFGKKT between TMDs 8 and 9,

LLPWSMLPDVIDDF in the loop between TMDs 10 and 11, YVFFTK in TMD 11, and LGVSTLSLDFA between TMDs 11 and 12.

Subcellular localization of Mfsd2a

Since the domain structure predicted that Mfsd2a is a membrane-associated protein, we determined with which membrane it was associated. To examine the subcellular localization of Mfsd2a, BAT cells were transfected with pCMV-Mfsd2a-FLAG encoding Mfsd2a fused to a 3xFLAG tag at its C-terminus. The localization of the Mfsd2a-FLAG was subsequently examined by confocal microscopy and compared to that of markers of mitochondria, lysosomes, and the ER. As shown in Figure 2, Mfsd2a co-localized with the ER marker rather than with markers for mitochondria and lysosomes. In addition, little Mfsd2a appeared to be localizing to the plasma membrane. Similar results were obtained with COS-1 cells (not shown). These results suggest that under the conditions analyzed, Mfsd2a is largely associated with the ER. Consistent with this, Mfsd2a contains 4 putative ER localization signals (consensus: KKXX; Supplementary Figure S1A) [24], one of which is conserved between human and mouse Mfsd2a.

Tissue-specific pattern of *Mfsd2a* mRNA expression

To examine the tissue-specific expression of *Mfsd2a*, Northern blot analysis was performed using total RNA isolated from multiple adult mouse tissues (Figure 3A). The *Mfsd2a* cDNA probe hybridized to an mRNA of about 2.2 kb in size. *Mfsd2a* mRNA was expressed in many tissues; the highest level of expression was observed in brain, intestine, kidney, liver, lung, mammary gland, and prostate. Compared to *Mfsd2a*, *Mfsd2b* was expressed in few tissues and at relatively low levels (Supplementary Figures S2A, B). Highest expression of *Mfsd2b* was detected in spleen, followed by lung and testis.

As mentioned above, *Mfsd2a* was originally identified by gene expression profiling as a gene up-regulated in BAT from DKO mice (see Material and Methods section under Microarray analysis). To validate this observation, *Mfsd2a* expression was compared between BAT from WT and DKO mice. As shown in Supplementary Figure S2C, *Mfsd2a* was expressed in BAT of DKO mice at a >15-fold higher level compared to that of WT mice.

Mfsd2a follows a circadian expression pattern

Examination of the level *Mfsd2a* mRNA expression over a period of 24 h showed that *Mfsd2a* expression displayed an oscillatory expression profile in BAT and liver (Figure 3B). The expression of *Mfsd2a* steadily increased during the light cycle, reached its zenith around CT12, and then rapidly decreased during the early phase of the dark cycle. The periodicity was identical for BAT and liver. These data show that *Mfsd2a* exhibits an oscillatory expression pattern consistent with a circadian rhythm.

Induction of *Mfsd2a* expression during adaptive thermogenesis and fasting

To gain further insight into the function of Mfsd2a in BAT, we examined whether it might have a role in adaptive thermogenesis. Therefore, WT mice were exposed to an ambient temperature of 4°C and, at different times during cold exposure BAT, mRNA was isolated and *Mfsd2a* expression examined by qRT-PCR. As shown in Figure 4A, *Mfsd2a* mRNA expression was dramatically induced in a time-dependent manner in BAT during cold exposure similar to *Dio2* and *Ucp1* expression, genes known to be induced during thermogenesis [6, 7, 9]. This dramatic induction of *Mfsd2*a was confirmed by Northern blot analysis (Figure 4B). These data demonstrate that in BAT increased *Mfsd2a* expression is associated with adaptive thermogenesis suggesting a function for Mfsd2a in this process. Cold exposure did not change

the expression of *Mfsd2a* in liver, kidney, and skeletal muscle or that of *Mfsd2b* in BAT significantly (data not shown).

Previous studies have demonstrated that activation of βARs plays a key role in driving adaptive thermogenesis in BAT [4,10]. Therefore, we compared the induction of *Mfsd2a* expression during thermogenesis between WT and βAR-less mice. QRT-PCR analysis showed that, as *Ucp1* and *Dio2* expression, the induction of *Mfsd2a* was greatly reduced in BAT from β-less upon cold exposure (Figure 4C). These results suggest that activation of βARs plays a critical role in the regulation of *Mfsd2a* expression during adaptive thermogenesis. To obtain further support for this concept, mice were treated with the βAR pan-agonist isoproterenol or the β3-specific agonist CL316243 and their effect on *Mfsd2a* expression examined. As shown in Figure 4D, both isoproterenol and CL316243 significantly increased the expression of *Mfsd2a*. *Mfsd2a* expression was increased to a greater extent than that of *Ucp1* and *Dio2*. These results support the hypothesis that the induction of *Mfsd2a* during adaptive thermogenesis is dependent on activation of the β-adrenergic signaling pathway.

A number of genes that are induced during adaptive thermogenesis, have been reported to also be up-regulated during fasting, another process that involves the release of energy from stored fatty acids or carbohydrates [25,26]. We, therefore, were interested in determining whether *Mfsd2a* expression was also enhanced during fasting. As shown in Figure 4E, the expression of *Mfsd2a* was highly induced in both BAT and liver after fasting.

Regulation of *Mfsd2a* expression in cultured brown adipocytes

To obtain further insights into the role of Mfsd2a in brown adipocytes, we examined whether *Mfsd2a* expression was altered during differentiation of cultured BAT cells. As shown in Figure 5A, *Mfsd2a* was expressed at relatively low levels in pre-adipocytes, and its expression levels remained unchanged during their differentiation into brown adipocytes. In contrast, the brown adipocyte marker *Ucp1* was highly induced during brown adipocyte differentiation [7, 14].

The results in Figures 4C and D showed that the induction of *Mfsd2a* expression during thermogenesis was dependent on the activation of βAR. Activation of the βAR signaling pathway results in an increase in cAMP levels and activation of Protein Kinase A (PKA) that subsequently leads to the phosphorylation and activation of several transcriptional mediators, and the induction of several thermogenic marker genes. The latter can be reproduced in cultured differentiated BAT cells by the addition of dibut-cAMP [4, 8, 10]. We therefore examined the effect of cAMP on *Mfsd2a* expression. As shown in Figure 5B, treatment of fully differentiated BAT cells with dibut-cAMP induced expression of *Mfsd2a* in a time-dependent manner as reported for *Ucp1*. *Mfsd2a* expression was induced 10-fold 2 hr after the addition of dibut-cAMP. Treatment of BAT cells with NE (Figure 5B) also enhanced *Mfsd2a* mRNA expression. Addition of dibut-cAMP to preadipocytes did not induce Mfsd2a expression (data not shown).

Previous studies have shown that about 32% of the genes induced by cAMP in BAT cells, including *UCP1*, are dependent on PGC-1α [14]. As shown in Figure 5C, the induction of *Mfsd2a* in PGC-1α$^{-/-}$ BAT cells by cAMP was not significantly different from that in WT cells. These results suggest that the induction of *Msfd2a* is independent of PGC-1α expression.

DISCUSSION

In this study, we describe the identification of a novel subfamily of major facilitator domain-containing proteins, not reported previously, and referred to as Mfsd2. Murine *Mfsd2a* was identified as a gene up-regulated in BAT of mice deficient in the expression of the nuclear receptors RORα and RORγ. Sequence analysis discovered a closely related protein, referred to as Mfsd2b, that exhibited a ~60% similarity with Mfsd2a. Their highly conserved genomic

structure suggests that *Mfsd2a* and *Mfsd2b* belong to the same subfamily and are derived from the duplication of an ancestral gene. In addition, sequence comparison identified a *Xenopus*and two zebrafish homologs of Mfsd2 that, based on sequence similarity, were more closely related to Mfsd2a than to Mfsd2b. The Mfsd2 proteins exhibited a 43-47% sequence similarity with the Na^+/melibiose symporter MelB and related carbohydrate transporters [18-20].

The structure of MelB has been extensively studied [18,19,22,23,27]. These topological analyses demonstrated the presence of 12 α-helical transmembrane spanning segments. Secondary structure analysis of Mfsd2 proteins predicted the presence of 12 putative α-helical TMDs (Figure 1). Comparison of the sequence with that of MelB supported the conclusion that these proteins likely contain 12 TMDs. The latter is in agreement with the observations showing that many members of the major facilitator/permease superfamily contain 12 TMDs [28]. However, based on their sequence homology, Mfsd2 proteins are only distantly related to other mammalian major facilitator domain-containing proteins, including members of the GLUT family, as the Mfsd2 proteins do not contain any of the conserved sequences characteristic of the GLUT family [28,29].

Recent studies have shown that the cytoplasmic loop between helixes 4 and 5 of MelB is functionally important [22]. Mutation of the amino acids R141 or E142 within this loop greatly impairs the Na+/sugar translocation; however, these mutants retain their sugar binding capacity. Interestingly, these two amino acids are conserved between MelB and Mfsd2 proteins. In addition, several of the amino acids that are essential for cation binding/recognition in MelB, including Asp-55, Asn-58 and Asp-59, are conserved in Mfsd2 proteins. These similarities further support the hypothesis that Mfsd2 proteins might function as cation/carbohydrate symporters. Although many carbohydrate transporters localize to the plasma membrane and Mfsd2a was found to be largely associated with the ER, the trafficking of several transporters from intracellular compartments to the plasma membrane is under strict control. For example, insulin stimulates the translocation of GLUT4 to the plasma membrane whereas activation of βAR promotes accumulation into intracellular compartments [30,31]. A good antibody is needed to determine what the distribution is of endogenous Mfsd2a and whether the subcellular localization of Mfsd2a is regulated in a similar manner.

Mfsd2a was found to be expressed in many tissues. In BAT and liver *Mfsd2a* displayed an oscillatory expression profile consistent with a circadian rhythm (Figure 3C). *Mfsd2a* mRNA expression reached its highest level at the end of the light cycle at CT12 and then rapidly decreased. Previously, we reported that in BAT *RORα1* and *RORγ1* also exhibit an oscillatory expression profile [16]. Interestingly, expression of *Mfsd2a* decreases at a time when the expression of *RORα1* and *RORγ1* increases. This suggested that RORs might function as repressors of *Mfsd2a* expression. Consistent with this concept is the observation that *Mfsd2a* is up-regulated in BAT from DKO mice (Figure 3B).

Because *Mfsd2a* was identified as a gene up-regulated in BAT from DKO mice, we were particularly interested in its expression and function in this tissue. *Mfsd2a* is expressed at relatively low levels in BAT and in cultured pre-adipocytes. The expression of *Mfsd2a* remains unchanged during differentiation of pre-adipocytes into fully differentiated BAT cells (Figure 5A) suggesting that Mfsd2a does not play a major role during differentiation. However, our data demonstrated that *Mfsd2a* was highly induced in BAT during cold-induced thermogenesis suggesting that *Mfsd2a* has a function in BAT during adaptive thermogenesis. Previous studies have shown that cold-induced thermogenesis is dependent on β-adrenergic stimulation [5, 15]. The induction of genes normally induced during thermogenesis, including *Ucp1* and *Dio2* [4-7, 9, 14], is greatly diminished in mice deficient in the three βARs. Our results show that *Mfsd2a* expression is not greatly increased upon cold exposure in BAT of β-less mice

suggesting that activation of the β-adrenergic signaling pathway plays a major role in the induction of *Mfsd2a* expression during adaptive thermogenesis. This further supported by data showing that treatment with βAR agonists induced *Mfsd2a* expression in WT mice but not in β-less mice.

Activation of the βAR leads to an increase in cAMP levels and activation of PKA followed by phosphorylation and activation of various transcription factors that subsequently enhance the transcription of thermogenic genes [4,8,10]. This action is mimicked in cultured differentiated BAT cells by treatment with dibut-cAMP or NE, an activator of βAR. Our results demonstrated that treatment of BAT cells with dibut-cAMP or cAMP-inducing agents greatly induced the expression of *Mfsd2a*. These observations support the hypothesis that the regulation of *Mfsd2a* expression during thermogenesis is at least in part dependent on the activation of βAR and PKA signaling. The precise molecular mechanisms involved in the induction of gene expression during adaptive thermogenesis are not yet fully understood. Nuclear receptors PPARs, T3R, and ERRα, the co-activator PGC-1α, the transcription factors NRF1/2 and CREB have been implicated in the regulation of various genes during thermogenesis [4,8,10,12,32]. Activation of PKA mediates the activation of CREB, which in turn enhances the transcription of a number of genes, including PGC-1α and DIO2. PGC-1α functions as a co-activator for a number of nuclear receptors, including PPARs and ERRα, as well as NRF1. A recent study showed that PGC-1α is required for 32% of the genes induced in BAT by cAMP [14]. Our results show that the induction of *Mfsd2a* is independent of PGC-1α. Future studies have to determine the precise molecular mechanism that regulates Mfsd2a transcription.

Glucose uptake is markedly enhanced in BAT during cold exposure and is dependent on activation of the βAR pathway [33,34]. It is interesting to note that the induction of Mfsd2a during thermogenesis resembles that of the glucose transporter GLUT1 (SLC2A1). As Mfsd2a, GLUT1 expression is also induced in BAT *in vitro* and *in vivo* by βAR stimulation [31,33]. In contrast, GLUT4 expression is down-regulated after treatment with βAR agonists. These observations suggest distinct regulation and roles of different sugar transporters in thermogenesis. It is believed that GLUT1 is responsible for a large portion of the increase in glucose uptake observed during cold exposure. Whether Mfsd2a contributes to the increased uptake of sugars during adaptive thermogenesis needs to be determined. Identification of the molecules transported by Mfsd2a will be necessary to understand the physiological functions of Mfsd2a.

In summary, in this study we describe a new subfamily of major facilitator proteins that is closely related to the bacterial Na^+/melibiose symporter MelB. We provide evidence showing that in BAT *Mfsd2a* is dramatically induced during adaptive thermogenesis cold exposure suggesting that Mfsd2a has a specific role in BAT during adaptive thermogenesis. We demonstrate that activation of the β-AR signaling pathway, but not PGC-1α, plays a major role in this induction.

Supplementary Material

Refer to Web version on PubMed Central for supplementary material.

ACKNOWLEDGMENTS

The authors would like to thank Drs. John Pritchard and Jennifer Perry for their valuable comments on the manuscript, Laura Miller for her assistance with the mice, and Dr. Xiying Wu for his assistance with the circadian rhythm analysis. This research was supported by the Intramural Research Program of the NIEHS, NIH (Z01-ES-101586) (AMJ) and by a CNRU Center Grant # 1P30 DK072476 entitled “Nutritional Programming: Environmental and Molecular Interactions” sponsored by NIDDK (J.M.G.).

Abbreviations

Mfsd2a, major facilitator superfamily domain-containing protein 2a; TG, triglycerides; βAR, beta-adrenergic receptor; ROR, retinoid-related orphan receptor; BAT, brown adipose tissue; WAT, white adipose tissue; NE, norepinephrine.

REFERENCES

1. Klaus S. Adipose tissue as a regulator of energy balance. Curr. Drug Targets 2004;5:241–250. [PubMed: 15058310]
2. Rosen ED, Spiegelman BM. Molecular regulation of adipogenesis. Annu. Rev. Cell. Dev. Biol 2000;16:145–171. [PubMed: 11031233]
3. Scherer PE. Adipose tissue: from lipid storage compartment to endocrine organ. Diabetes 2006;55:1537–1545. [PubMed: 16731815]
4. Cannon B, Nedergaard J. Brown adipose tissue: function and physiological significance. Physiol. Rev 2004;84:277–359. [PubMed: 14715917]
5. Lowell BB, Bachman ES. Beta-Adrenergic receptors, diet-induced thermogenesis, and obesity. J. Biol. Chem 2003;278:29385–29388. [PubMed: 12788929]
6. Golozoubova V, Cannon B, Nedergaard J. UCP1 is essential for adaptive adrenergic nonshivering thermogenesis. Am. J. Physiol. Endocrinol. Metab 2006;291:E350–357. [PubMed: 16595854]
7. Kozak LP, Harper ME. Mitochondrial uncoupling proteins in energy expenditure. Annu. Rev. Nutr 2000;20:339–363. [PubMed: 10940338]
8. Robidoux J, Martin TL, Collins S. Beta-adrenergic receptors and regulation of energy expenditure: a family affair. Annu. Rev. Pharmacol. Toxicol 2004;44:297–323. [PubMed: 14744248]
9. de Jesus LA, Carvalho SD, Ribeiro MO, Schneider M, Kim SW, Harney JW, Larsen PR, Bianco AC. The type 2 iodothyronine deiodinase is essential for adaptive thermogenesis in brown adipose tissue. J. Clin. Invest 2001;108:1379–1385. [PubMed: 11696583]
10. Lowell BB, Spiegelman BM. Towards a molecular understanding of adaptive thermogenesis. Nature 2000;404:652–660. [PubMed: 10766252]
11. Silvestri E, Schiavo L, Lombardi A, Goglia F. Thyroid hormones as molecular determinants of thermogenesis. Acta Physiol. Scand 2005;184:265–283. [PubMed: 16026419]
12. Villena JA, Hock MB, Chang WY, Barcas JE, Giguere V, Kralli A. Orphan nuclear receptor estrogen-related receptor alpha is essential for adaptive thermogenesis. Proc. Natl. Acad. Sci. U. S. A 2007;104:1418–1423. [PubMed: 17229846]
13. Lin J, Handschin C, Spiegelman BM. Metabolic control through the PGC-1 family of transcription coactivators. Cell Metab 2005;1:361–370. [PubMed: 16054085]
14. Uldry M, Yang W, St-Pierre J, Lin J, Seale P, Spiegelman BM. Complementary action of the PGC-1 coactivators in mitochondrial biogenesis and brown fat differentiation. Cell Metab 2006;3:333–341. [PubMed: 16679291]
15. Bachman ES, Dhillon H, Zhang CY, Cinti S, Bianco AC, Kobilka BK, Lowell BB. betaAR signaling required for diet-induced thermogenesis and obesity resistance. Science 2002;297:843–845. [PubMed: 12161655]
16. Kang HS, Angers M, Beak JY, Wu X, Gimble JM, Wada T, Xie W, Collins JB, Grissom SF, Jetten AM. Gene expression profiling reveals a regulatory role for ROR{alpha} and ROR{gamma} in Phase I and Phase II Metabolism. Physiol. Genomics 2007;31:281–294. [PubMed: 17666523]
17. Jetten AM, Joo JH. Retinoid-related orphan receptors (RORs): roles in cellular differentiation and development. Adv. Devel. Biol 2006;16:314–354.
18. Botfield MC, Naguchi K, Tsuchiya T, Wilson TH. Membrane topology of the melibiose carrier of Escherichia coli. J. Biol. Chem 1992;267:1818–1822. [PubMed: 1730719]
19. Pourcher T, Bibi E, Kaback HR, Leblanc G. Membrane topology of the melibiose permease of Escherichia coli studied by melB-phoA fusion analysis. Biochemistry (Mosc) 1996;35:4161–4168.
20. Yazyu H, Shiota-Niiya S, Shimamoto T, Kanazawa H, Futai M, Tsuchiya T. Nucleotide sequence of the melB gene and characteristics of deduced amino acid sequence of the melibiose carrier in Escherichia coli. J. Biol. Chem 1984;259:4320–4326. [PubMed: 6323466]

21. Barrett MP, Walmsley AR, Gould GW. Structure and function of facilitative sugar transporters. Curr. Opin. Cell Biol 1999;11:496–502. [PubMed: 10449337]
22. Meyer-Lipp K, Sery N, Ganea C, Basquin C, Fendler K, Leblanc G. The Inner Interhelix Loop 4-5 of the Melibiose Permease from Escherichia coli Takes Part in Conformational Changes after Sugar Binding. J. Biol. Chem 2006;281:25882–25892. [PubMed: 16822867]
23. Purhonen P, Lundback AK, Lemonnier R, Leblanc G, Hebert H. Three-dimensional structure of the sugar symporter melibiose permease from cryo-electron microscopy. J. Struct. Biol 2005;152:76–83. [PubMed: 16139519]
24. Teasdale RD, Jackson MR. Signal-mediated sorting of membrane proteins between the endoplasmic reticulum and the golgi apparatus. Annu. Rev. Cell Dev. Biol 1996;12:27–54. [PubMed: 8970721]
25. Patsouris D, Mandard S, Voshol PJ, Escher P, Tan NS, Havekes LM, Koenig W, Marz W, Tafuri S, Wahli W, Muller M, Kersten S. PPARalpha governs glycerol metabolism. J. Clin. Invest 2004;114:94–103. [PubMed: 15232616]
26. Lin J, Puigserver P, Donovan J, Tarr P, Spiegelman BM. Peroxisome proliferator-activated receptor gamma coactivator 1beta (PGC-1beta), a novel PGC-1-related transcription coactivator associated with host cell factor. J. Biol. Chem 2002;277:1645–1648. [PubMed: 11733490]
27. Abdel-Dayem M, Basquin C, Pourcher T, Cordat E, Leblanc G. Cytoplasmic loop connecting helices IV and V of the melibiose permease from Escherichia coli is involved in the process of Na+-coupled sugar translocation. J. Biol. Chem 2003;278:1518–1524. [PubMed: 12421811]
28. Wood IS, Trayhurn P. Glucose transporters (GLUT and SGLT): expanded families of sugar transport proteins. Br. J. Nutr 2003;89:3–9. [PubMed: 12568659]
29. Uldry M, Thorens B. The SLC2 family of facilitated hexose and polyol transporters. Pflugers Arch 2004;447:480–489. [PubMed: 12750891]
30. Bogan JS, McKee AE, Lodish HF. Insulin-responsive compartments containing GLUT4 in 3T3-L1 and CHO cells: regulation by amino acid concentrations. Mol. Cell. Biol 2001;21:4785–4806. [PubMed: 11416153]
31. Dallner OS, Chernogubova E, Brolinson KA, Bengtsson T. Beta3-adrenergic receptors stimulate glucose uptake in brown adipocytes by two mechanisms independently of glucose transporter 4 translocation. Endocrinology 2006;147:5730–5739. [PubMed: 16959848]
32. Silva JE. Thermogenic mechanisms and their hormonal regulation. Physiol. Rev 2006;86:435–464. [PubMed: 16601266]
33. Greco-Perotto R, Zaninetti D, Assimacopoulos-Jeannet F, Bobbioni E, Jeanrenaud B. Stimulatory effect of cold adaptation on glucose utilization by brown adipose tissue. Relationship with changes in the glucose transporter system. J. Biol. Chem 1987;262:7732–7736. [PubMed: 3584138]
34. Vallerand AL, Perusse F, Bukowiecki LJ. Stimulatory effects of cold exposure and cold acclimation on glucose uptake in rat peripheral tissues. Am. J. Physiol 1990;259:R1043–1049. [PubMed: 2240264]

Figure 1. Amino acid sequence alignment of Mfsd2a, Mfsd2b, and MelB

Amino acid sequence alignment of Mfsd2a and Mfsd2b of different species. (-) indicates sequence identity with mouse Mfsd2a; (.) indicates gap. Mouse (m), human (h), *Xenopus* (x), and zebrafish (z) sequences are compared with those of Na^+/melibiose symporter (MelB) of

Nostoc punctiforme (n) and *Escherichia coli* (e). The α-helices indicating the 12 putative transmembrane domains are shaded.

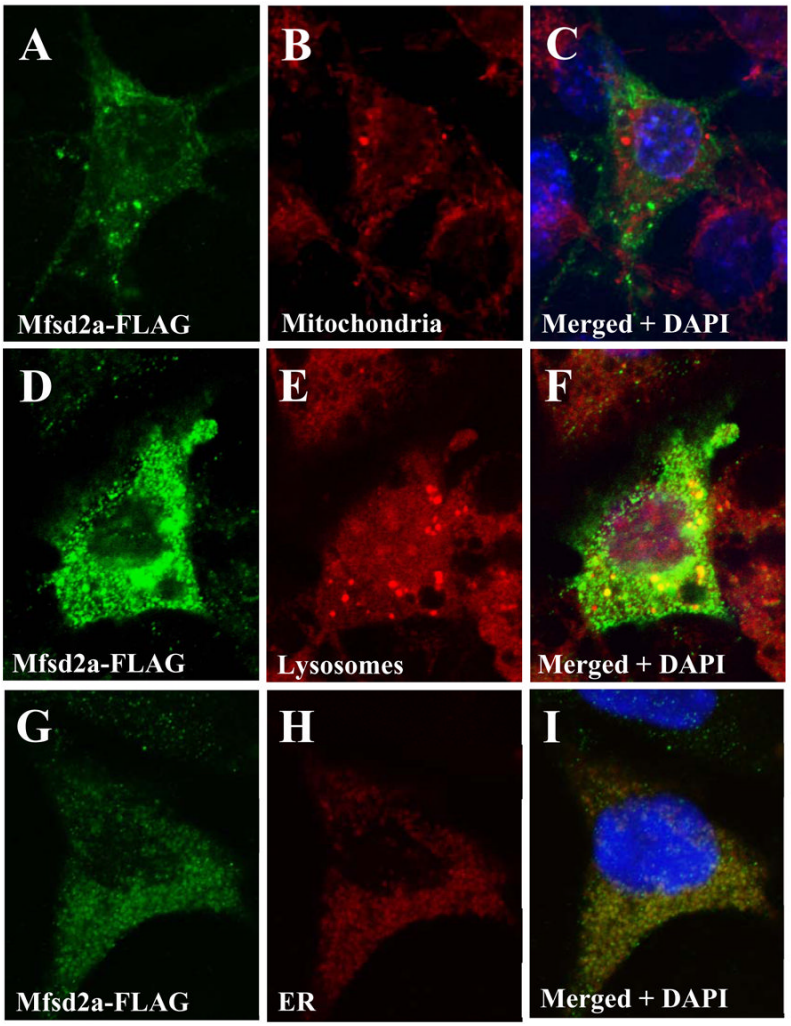

Figure 2. Mfsd2a protein is localized in the ER

Brown fat adipocytes were transfected with pCMV-Mfsd2a-FLAG. Forty-eight hours after transfection, the localization of Mfsd2a-FLAG protein was examined by confocal microscopy with a mouse anti-FLAG M2 antibody and Alexa 488 rabbit anti-mouse IgG. Mitochondria, lysozomes, ER, and nuclei were identified by MitoTracker Red CMX-Ros, LysoTracker Red, ER-targeted protein Red, and DAPI staining, respectively.

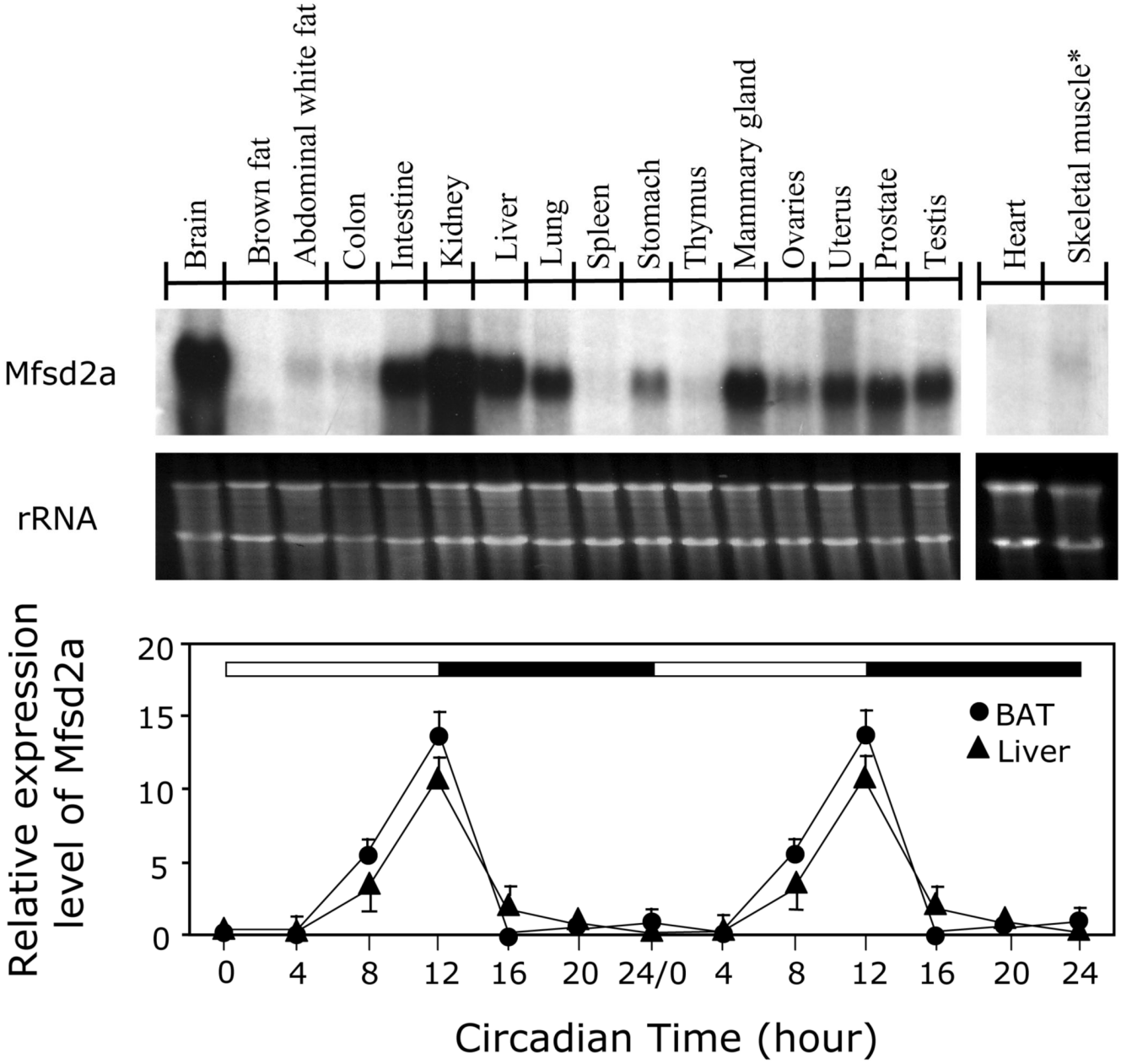

Figure 3. *Mfsd2a* has a wide tissue distribution and its expression oscillates through circadian time

(A) Tissue-specific pattern of expression of *Mfsd2a*. Total RNA isolated from multiple mouse tissues was examined by Northern blot analysis using a radio-labeled cDNA probe for *Mfsd2a*. Lower panel shows 18S and 28S rRNA stained with Ethidium Bromide (EtBr). *A combination of subscapular and teres major muscle. (B) *Mfsd2a* displays an oscillating expression profile. Total RNA from BAT and liver of male mice (n=4) was isolated over a 24 h period at the circadian time (CT) indicated. Subsequently the expression of *Mfsd2a* mRNA was examined by qRT-PCR analysis. Gene expression was normalized with the corresponding cyclophilin B levels and "double plotted" to display a duplicated 24 h profile. All values are reported as averages ± SE. The black and white bar indicates the light and dark period.

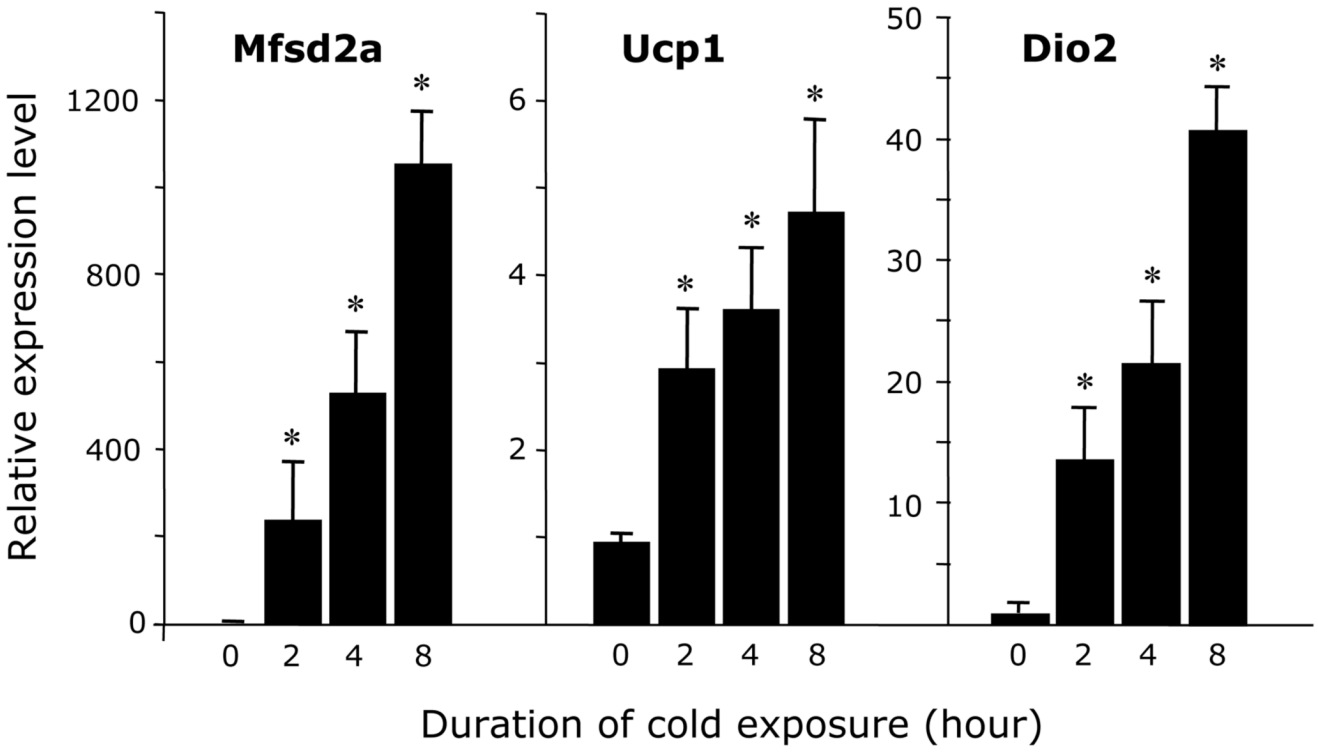

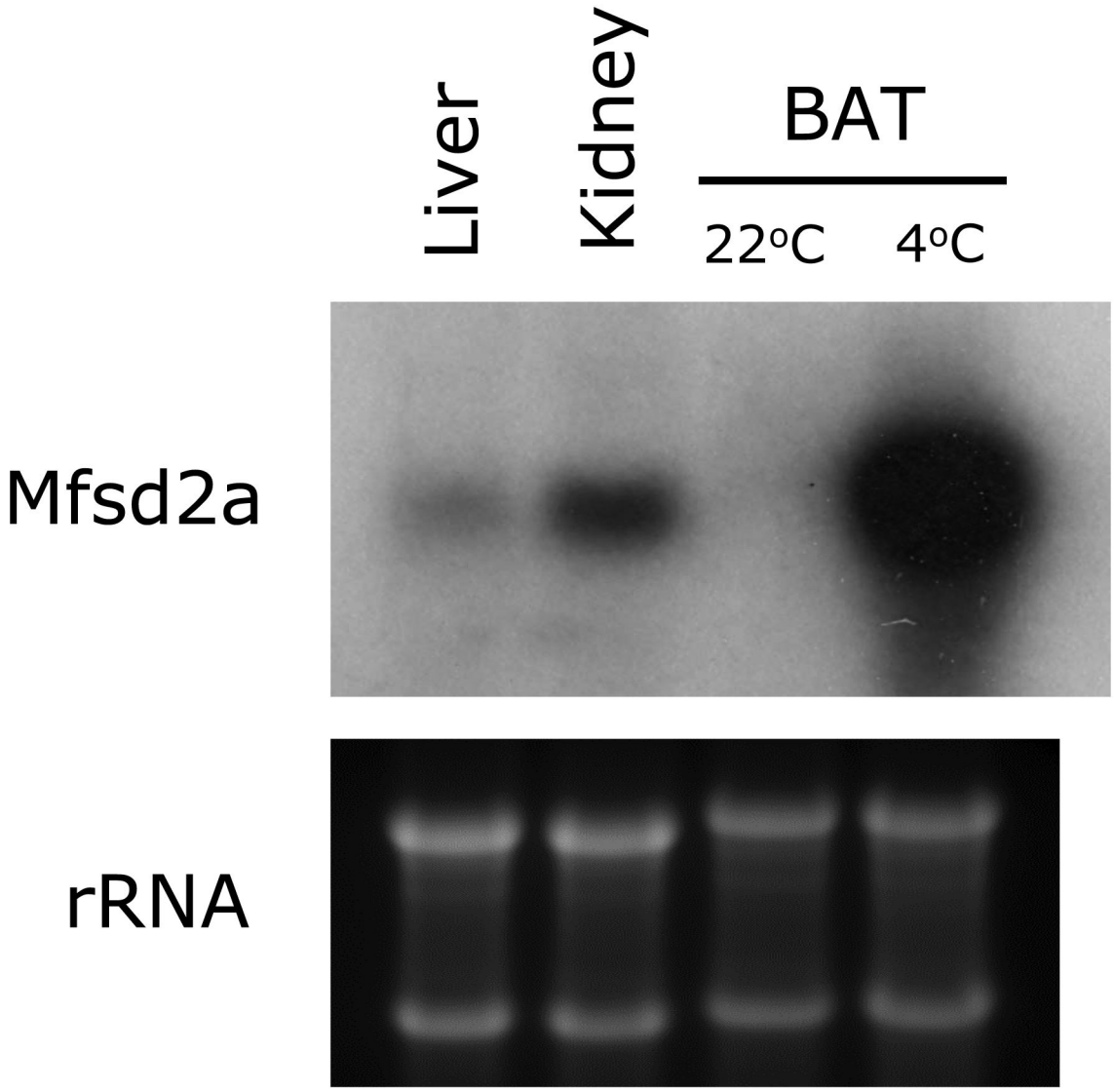

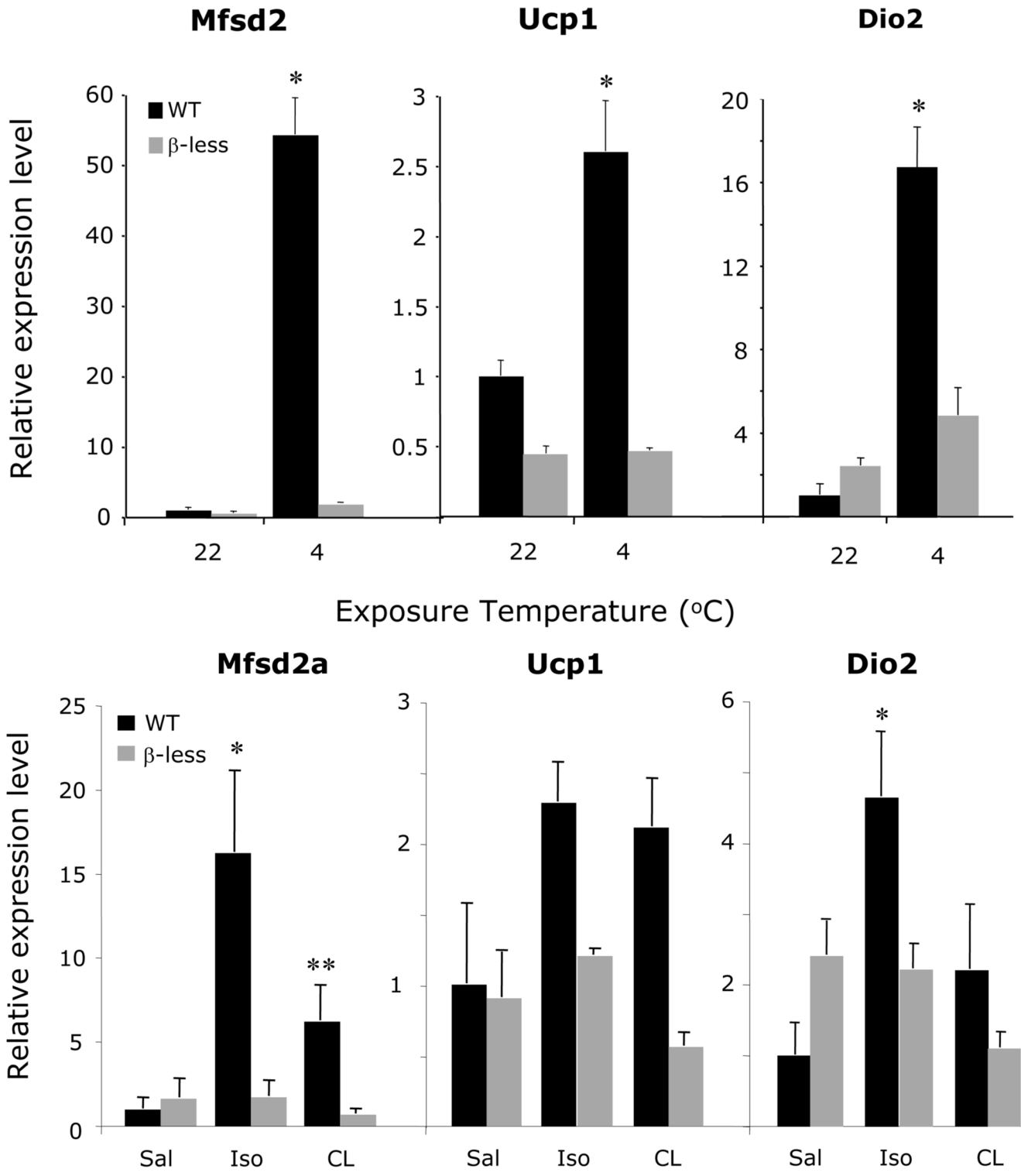

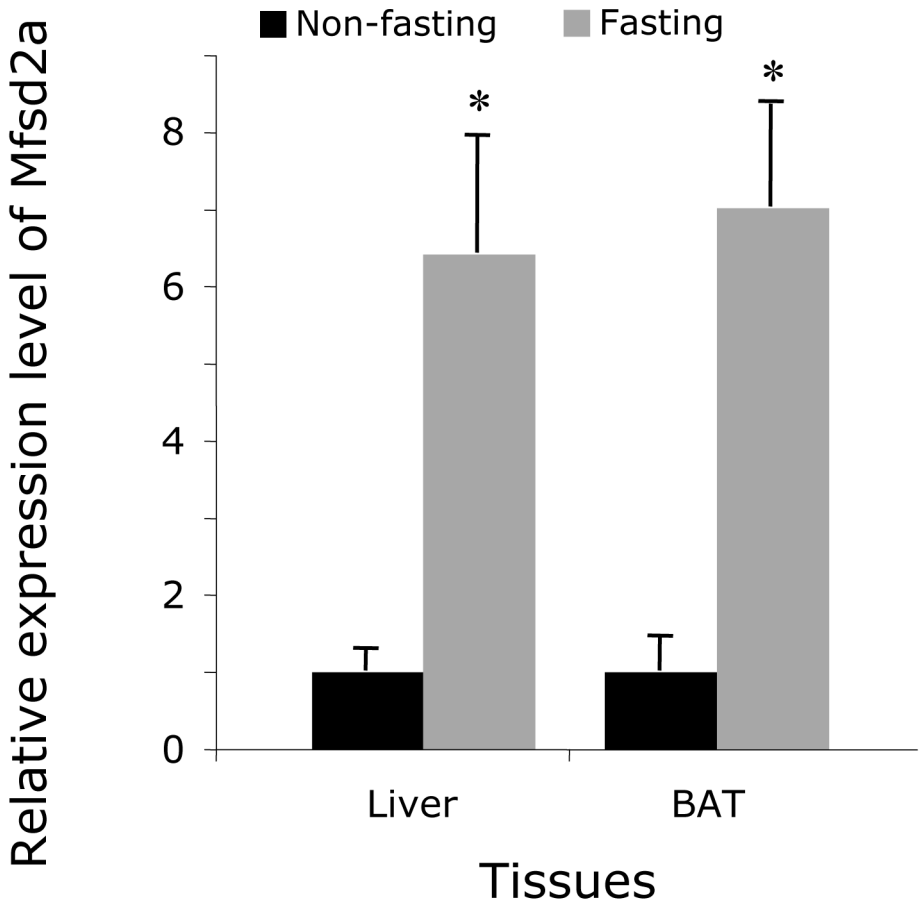

Figure 4. Mfsd2a expression is induced during adaptive thermogenesis and fasting

(A) *Mfsd2a* expression is greatly induced during adaptive thermogenesis. Mice (n=4) were subjected to a temperature of 4°C and BAT isolated at the time intervals indicated. The levels of *Mfsd2a*, *Ucp1*, and *Dio2* mRNA were assessed by qRT-PCR analysis. (B) Total RNA was isolated from the liver, kidney, and BAT (from mice kept at 22°C or 4°C for 8 h). *Mfsd2a* expression was examined by Northern blot analysis using a radiolabeled cDNA probe. Lower panel shows 18S and 28S rRNA. (C) Induction of *Mfsd2a* during thermogenesis is partially dependent on the activation of the βAR signaling pathway. WT and β-less mice (n=5) were placed at 4°C or room temperature (22°C). After 6 hrs, BAT was collected, total RNA isolated, and the level of *Mfsd2a* expression examined by qRT-PCR. (D) *Mfsd2a* is induced by β-adrenergic agonists. Total RNA was isolated from BAT of WT and β-less mice (n=5) treated with or without β-agonists (Sal, saline; Iso, isoproterenol; CL, CL316243) for 1 hour. The expression of *Mfsd2a*, *Ucp1*, and *Dio2* were examined by qRT-PCR analysis. (E) *Mfsd2a* expression is greatly induced in BAT and liver upon fasting (16 h). Total RNA was isolated from non-fasting and fasting WT mice (n=3) and then examined by qRT-PCR analysis. Relative abundance of mRNA was calculated after normalization to 18S rRNA. *$p<0.01$, **$p<0.05$.

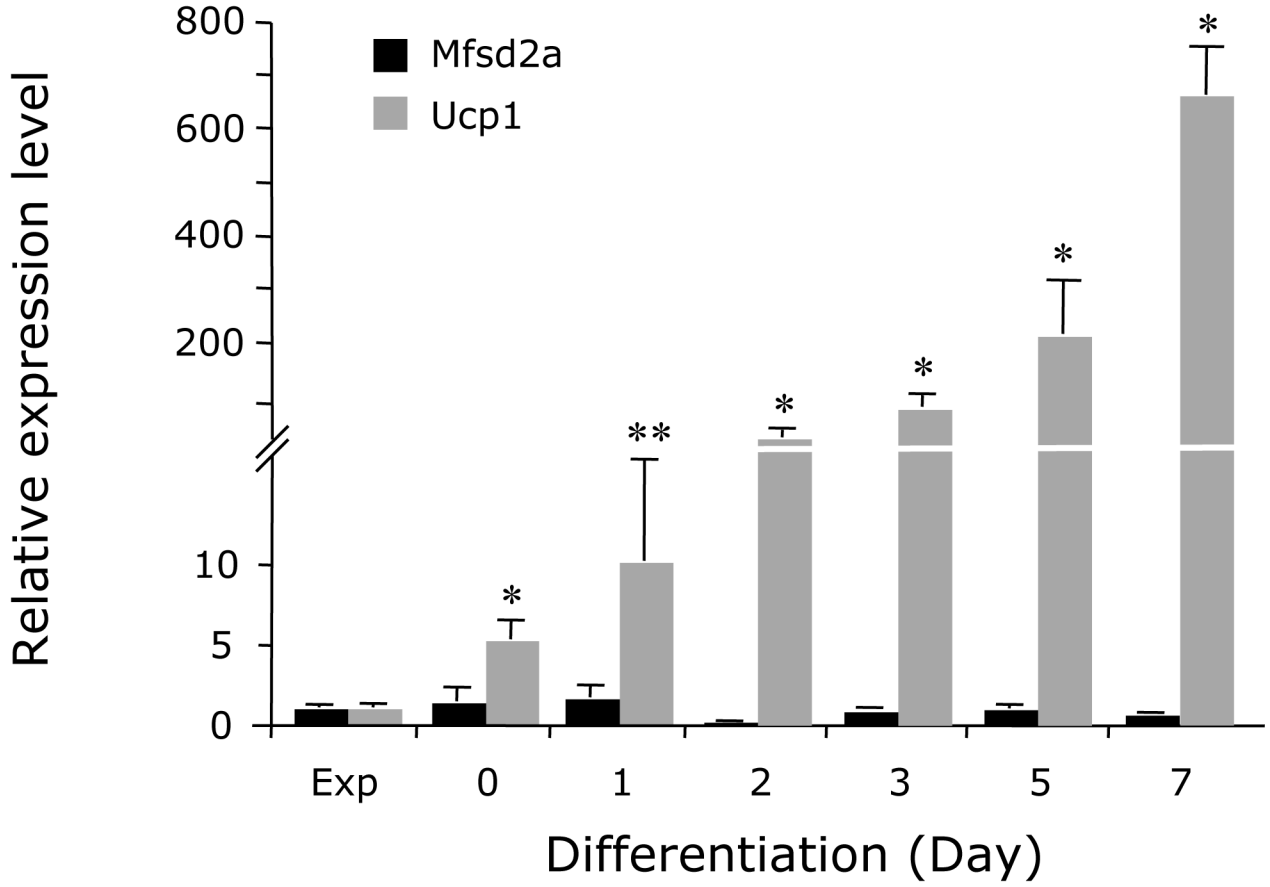

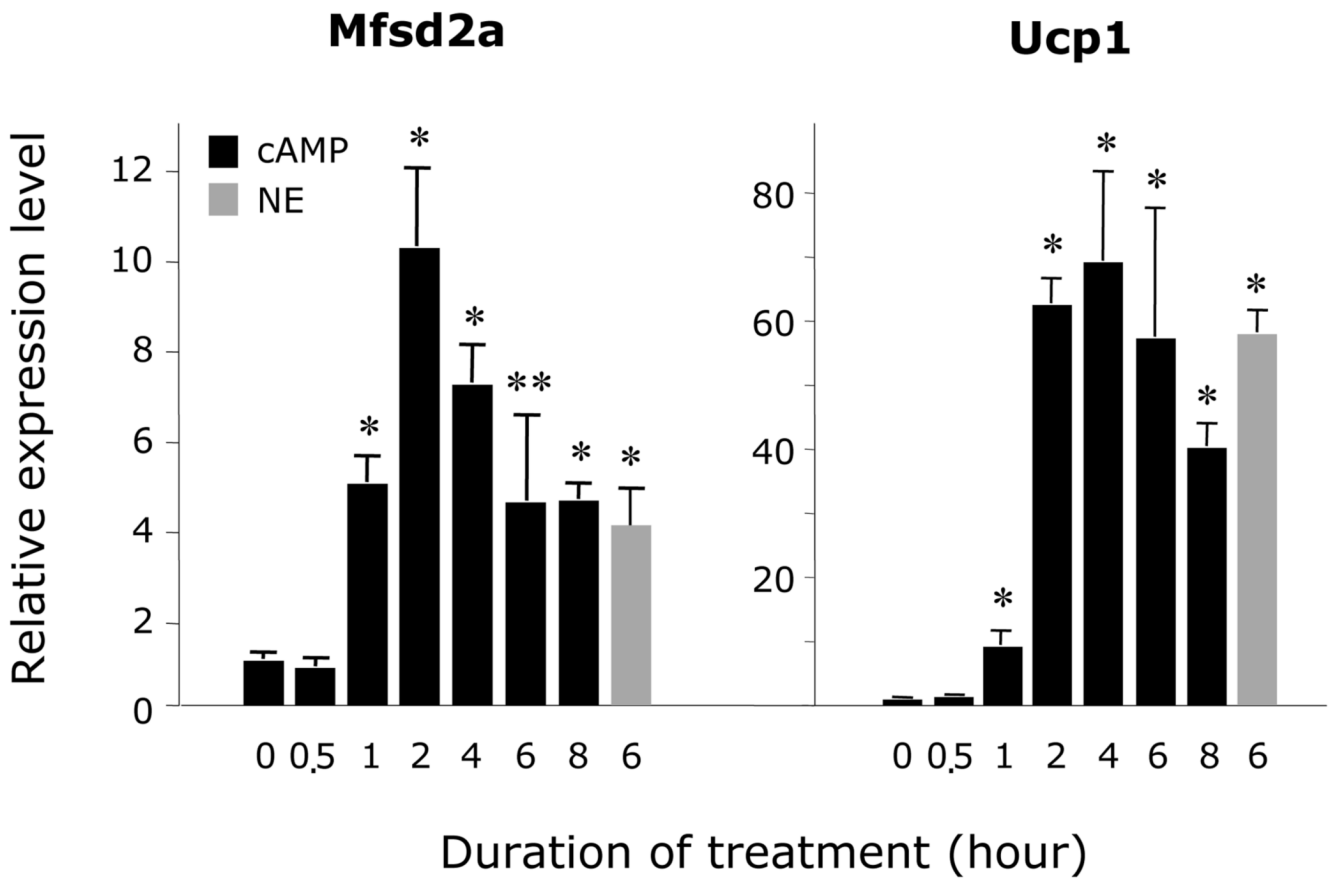

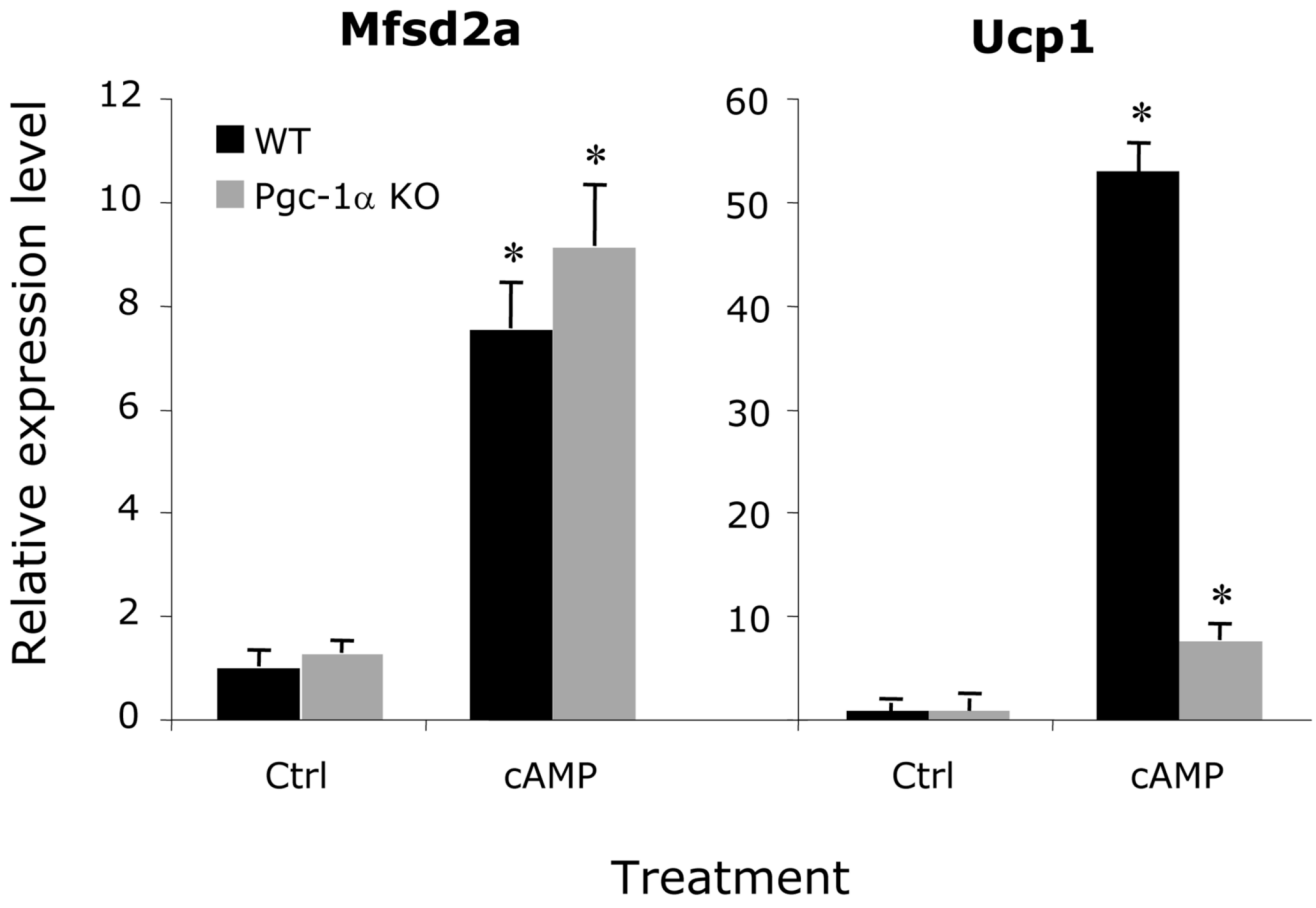

Figure 5. *Mfsd2a* expression does not change during BAT differentiation and is induced by dibut-cAMP

(A) *Mfsd2a* expression does not change during BAT differentiation. Pre-adipocytes were grown to confluence (day 0) and induced to differentiate into brown adipocytes as described in Materials and Methods. At the time intervals indicated cells were collected for RNA isolation. Expression of *Ucp1* and *Mfsd2a* mRNA were examined by qRT-PCR analysis. (Exp.) indicates cells were collected at the exponential growth phase. (B) Dibut-cAMP induces *Mfsd2a* expression in BAT cells. Fully differentiated brown adipocytes were treated with dibut-cAMP or NE and at different time intervals RNA was isolated and *Mfsd2a* and *Ucp1* expression examined by qRT-PCR. (C) Loss of PGC-1α expression does not abolish the induction of *Mfsd2a* expression by cAMP. Fully differentiated WT and PGC-1α-KO BAT cells were treated with dibut-cAMP. After 6 h of treatment, total RNA was isolated and the expression of *Mfsd2a* and *Ucp1* were examined by qRT-PCR analysis. Relative abundance of mRNA was calculated after normalization to 18S rRNA. *$p<0.01$, **$p<0.05$.